PASJ: Publ. Astron. Soc. Japan **64**, 22, 2012 April 25

X-Ray Groups of Galaxies at $0.5 < z < 1$ in zCOSMOS: Increased AGN Activities in High Redshift Groups

Masayuki TANAKA,[1] Alexis FINOGUENOV,[2] Simon J. LILLY,[3] Micol BOLZONELLA,[11] C. Marcella CAROLLO,[3] Thierry CONTINI,[4,5] Angela IOVINO,[6] Jean-Paul KNEIB,[7] Fabrice LAMAREILLE,[4,5] Olivier LE FEVRE,[7] Vincenzo MAINIERI,[8] Valentina PRESOTTO,[6] Alvio RENZINI,[9] Marco SCODEGGIO,[10] John D. SILVERMAN,[1] Gianni ZAMORANI,[11] Sandro BARDELLI,[11] Angela BONGIORNO,[2] Karina CAPUTI,[12] Olga CUCCIATI,[6] Sylvain DE LA TORRE,[12] Loic DE RAVEL,[12] Paolo FRANZETTI,[10] Bianca GARILLI,[10] Pawel KAMPCZYK,[3] Christian KNOBEL,[3] Katarina KOVAČ,[3,13] Jean-Francois LE BORGNE,[4,5] Vincent LE BRUN,[7] Carlos LÓPEZ-SANJUAN,[7] Christian MAIER,[3] Marco MIGNOLI,[11] Roser PELLO,[4,5] Yingjie PENG,[4,5] Enrique PEREZ-MONTERO,[4,5,14] Lidia TASCA,[7] Laurence TRESSE,[7] Daniela VERGANI,[11] Elena ZUCCA,[11] Luke BARNES,[3] Rongmon BORDOLOI,[3] Alberto CAPPI,[11] Andrea CIMATTI,[15] Graziano COPPA,[2] Anton M. KOEKEMOER,[16] Henry J. MCCRACKEN,[17] Michele MORESCO,[15] Preethi NAIR,[11] Pascal OESCH,[3] Lucia POZZETTI,[11] and Niraj WELIKALA[18]

[1]*Institute for the Physics and Mathematics of the Universe, The University of Tokyo, 5-1-5 Kashiwanoha, Kashiwa, Chiba 277-8583*
[2]*Max-Planck Institut für extraterrestrische Physik, Giessenbach-Strasse, D-85748 Garching bei München, Germany*
[3]*Institute of Astronomy, ETH Zürich, Zürich 8093, Switzerland*
[4]*Institut de Recherche en Astrophysique et Planétologie (IRAP), CNRS, 14, Avenue Edouard Belin, F-31400 Toulouse, France*
[5]*IRAP, Université de Toulouse, UPS-OMP, Toulouse, France*
[6]*INAF Osservatorio Astronomico di Brera, Via Brera 28, 20121 Milano, Italy*
[7]*Laboratoire d'Astrophyque de Marseille, CNRS/Aix-Marseille Université, 38 rue Frédéric Joliot-Curie, 13388, Marseille cedex 13, France*
[8]*European Southern Observatory, Karl-Schwarzschild-Strasse 2, D-85748 Garching bei München, Germany*
[9]*Dipartimento di Astronomia, Universita di Padova, vic. Osservatorio 3, I-35122 Padova, Italy*
[10]*INAF Institudo di Astrofísica Spaziale e Fisica Milano, Via E. Bassini 15, I-20133 Milano, Italy*
[11]*INAF Osservatorio Astronomico di Bologna, Via Ranzani 1, I-40127 Bologna, Italy*
[12]*Institute for Astronomy, University of Edinburgh, Royal Observatory, Blackford Hill, Edinburgh EH9 3HJ, UK*
[13]*Max-Planck Institut für Astrophysik, Karl-Schwarzschild-Strasse 1, D-85748 Garching bei München, Germany*
[14]*Instituto de Astrofísica de Andalucía, CSIC, Apartado de Correos 3004, 18080 Granada, Spain*
[15]*Dipartimento di Astronomia, Università degli Studi di Bologna, Via Ranzani 1, 40127 Bologna, Italy*
[16]*Space Telescope Science Institute, 3700 San Martin Drive, Baltimore, MD 2121, USA*
[17]*Institut d'Astrophysique de Paris, UMR7095 CNRS, Université Pierre & Marie Curie, 75014 Paris, France*
[18]*Insitut d'Astrophysique Spatiale, CNRS & Universit de Paris Sud-XI, 91405 Orsay cedex, France*

(Received 2011 June 24; accepted 2011 September 21)

Abstract

We present a photometric and spectroscopic study of galaxies at $0.5 < z < 1$ as a function of the environment based on data from the zCOSMOS survey. There is a fair amount of evidence that galaxy properties depend on the mass of groups and clusters, in the sense that quiescent galaxies prefer more massive systems. We base our analysis on a mass-selected environment using X-ray groups of galaxies, and define the group membership using a large number of spectroscopic redshifts from zCOSMOS. We show that the fraction of red galaxies is higher in groups than in the field at all redshifts probed in our study. Interestingly, the fraction of [O II] emitters on the red sequence increases at higher redshifts in groups, while the fraction does not strongly evolve in the field. This is due to increased dusty star-formation activities and/or increased activities of active galactic nuclei (AGNs) in high-redshift groups. We investigate these possibilities using the 30-band photometry and X-ray data. We find that the stellar population of the red [O II] emitters in groups is old, and there is no clear hint of dusty star-formation activities in those galaxies. The observed increase of red [O II] emitters in groups is likely due to increased AGN activities. However, since our overall statistics are poor, any firm conclusions need to be drawn from a larger statistical sample of $z \sim 1$ groups.

Key words: galaxies: clusters: general — galaxies: evolution — galaxies: fundamental parameters — surveys

1. Introduction

The matter distribution in the early universe was nearly uniform, but not completely so, and small density fluctuations grew with time through gravitational forces. Eventually, matter became dense enough to initiate star formation, and galaxies formed in high-density peaks of the density fluctuations. Galaxies grew progressively more massive by accreting

material from the surroundings, and by merging with other galaxies. The cosmic large-scale structure, in which galaxies are embedded, also developed with time. Later on, clusters of galaxies formed at the nodes of filaments, where galaxies could be quenched by gravitational and gas-dynamical effects. The evolution of galaxies and large-scale structure proceeded in tandem, and galaxies eventually acquired the properties that we observe today. This current framework of galaxy formation and evolution indicates that the formation and evolution of galaxies are driven by statistical events (e.g., they form in density fluctuations and grow by mergers) and that galaxies are statistical objects in nature. They do not form at the same time and they do not evolve in the same way. Only by statistical analyses can we study the physics of galaxy formation and evolution.

This fundamental principle has motivated a number of galaxy surveys. Imaging surveys deliver limited information about galaxy properties because one needs precise distances to galaxies in order to translate the observed quantities into physical quantities. For this reason, several large spectroscopic surveys have been carried out to date, and they have yielded new insights into galaxy evolution on the cosmological time scale.

The Harvard-Smithsonian Center for Astrophysics (CfA) redshift survey was the first systematic spectroscopic survey of the local universe in the late 1970's (Geller & Huchra 1989). It measured the redshifts of nearby galaxies, and revealed the cosmic large-scale structure in the local universe, making major progress in our understanding of the galaxy distribution in our universe. Following the CfA redshift survey, the Las Campanas redshift survey (Shectman et al. 1996) mapped out the galaxy distribution to larger distances, and the Canada-France redshift survey (Lilly et al. 1995) reached up to $z = 1$. The Sloan Digital Sky Survey (SDSS: York et al. 2000) and the 2-degree field redshift survey (2dF: Colless et al. 2003) surpassed the previous surveys with much improved statistics. In particular, SDSS imaged a quarter of the sky in five photometric bands (Fukugita et al. 1996; Doi et al. 2010) and measured more than 2 million redshifts with unprecedented precision (Aihara et al. 2011). SDSS dramatically refined our view of the local universe. In parallel with these surveys of the local universe, large spectroscopic surveys with 8m telescopes, such as DEEP2 (Davis et al. 2003), VIMOS VLT Deep Survey (Le Fèvre et al. 2005), and zCOSMOS (Lilly et al. 2007), peered deep into the universe reaching $z > 1$. All of these surveys enabled statistical analyses of galaxy populations in a large redshift range, yielding new insights into the evolution of galaxies. This paper is in the context of such statistical galaxy studies from large spectroscopic surveys. We will consider galaxy properties up to $z = 1$ using data from zCOSMOS with particular emphasis on the dependence of galaxy properties on the environment.

Pioneering work on this subject was made by Dressler (1980), who first quantified the morphology–density relation. Following this work, many authors studied the relation between galaxy properties and the environment (e.g., Postman & Geller 1984; Whitmore et al. 1993; Balogh et al. 1997; Dressler et al. 1997; Poggianti et al. 1999; see Tanaka et al. 2005 for a thorough set of references and also see more recent papers below). The SDSS and 2dF data sets delivered unprecedented statistics, and we now have a fairly good understanding of galaxy properties in the local universe (Lewis et al. 2002; Gómez et al. 2003; Blanton et al. 2003; Goto et al. 2003; Kauffmann et al. 2004; Tanaka et al. 2004; Blanton et al. 2005; Baldry et al. 2006). The advent of 8m-class telescopes pushed those environment studies to redshifts of unity and over (Rosati et al. 1999; Kodama et al. 2001; Lubin et al. 2002; Demarco et al. 2005; Nakata et al. 2005; Tanaka et al. 2005, 2010a, 2010b; Stanford et al. 2005, 2006; Poggianti et al. 2006, 2008; Demarco et al. 2007; Koyama et al. 2007; Fassbender et al. 2008; Lidman et al. 2008; Mei et al. 2009; Rettura et al. 2010; Strazzullo et al. 2010; Bauer et al. 2011). However, many of these high-z studies still suffer from limited statistics, particularly in low-medium density environments, which are the area where large spectroscopic surveys fill in, since they mainly probe such environments (Cucciati et al. 2006, 2010; Cooper et al. 2007, 2010; Tasca et al. 2009; Bolzonella et al. 2010; Iovino et al. 2010).

However, results from these deep surveys and their interpretations are not always consistent. In particular, the dependence of galaxy colors on the environment at $z \sim 1$ is controversial, as discussed in Cooper et al. (2010). There are a number of differences between the data sets from different surveys and the ways in which the analyses are made, which might explain the possible inconsistency. In this paper, we consider photometric and spectroscopic properties of galaxies as a function of the environment, and make an attempt to settle the issue. A unique feature of our study is that we define mass-selected environments using X-ray groups. Most of the previous studies are based on the environment traced by galaxies, where there is room for observational biases to enter. Such biases include the sampling rate, redshift success rate as functions of the redshift and galaxy type, large-scale structure, etc. For example, if a sample is biased toward star-forming galaxies, which can be the case at high redshifts in optical surveys, the density field traced by galaxies is basically the density of star-forming galaxies, which may not represent the true underlying density field. X-rays, on the other hand, are free from such biases. An extended X-ray emission is a strong signature of a dynamically bound system. Also, the X-ray luminosity is a good proxy for the mass of a system, making it possible to define environments by mass. We present a robust analysis of the dependence of galaxy properties on the environment based on a stellar mass-limited galaxy sample with mass-selected environments.

The structure of this paper is as follows. We briefly summarize the zCOSMOS survey and make an X-ray group catalog in section 2. We then consider the properties of the group galaxies, and make comparisons with field galaxies in section 3. Section 4 discusses the results and the paper is concluded in section 5. Unless otherwise stated, we use $\Omega_{\rm M} = 0.26$, $\Omega_\Lambda = 0.74$, and $\rm H_0 = 72\,km\,s^{-1}\,Mpc^{-1}$. The uncertainties are given in 68% confidence intervals. All of the magnitudes are given in the AB system.

2. X-Ray Group and Member Galaxy Catalogs

We consider the spectroscopic property of galaxies up to $z = 1$ based on data from the zCOSMOS survey (Lilly et al.

2007). We first briefly describe the survey, and then move on to making a catalog of galaxy groups selected from deep X-ray data.

2.1. The zCOSMOS Redshift Survey

The zCOSMOS is a spectroscopic survey of the COSMOS field (Scoville et al. 2007; Koekemoer et al. 2007) using the VIMOS spectrograph on the Very Large Telescope (VLT) on the Cerro Paranal (Le Fèvre et al. 2003). It is the largest program ever conducted at VLT with 600 hr of allocated time. The survey consists of two components: zCOSMOS-bright and zCOSMOS-faint. The former is a flux-limited survey down to $I_{\rm AB} = 22.5$ using a medium-resolution grism ($R \sim 500$) with a wavelength range of 5550–9650 Å. The latter is a color-selected galaxy survey aiming at $z \sim 2$ galaxies using a low-resolution blue grism with $R \sim 200$ ranging over 3700–6700 Å. All of the spectra were visually inspected by two people independently, and the final redshifts and confidence flags were determined in the meetings of face-face reconciliation. In this study, we used the zCOSMOS-bright 20k data to perform statistical analyses of galaxy groups. For further details about the survey, the reader is referred to Lilly et al. (2007, 2009).

2.2. X-Ray Group Catalog

We made an X-ray group catalog using X-ray data from XMM-Newton and Chandra available in the COSMOS field (Hasinger et al. 2007; Elvis et al. 2009). An early version of the group catalog was presented in Finoguenov et al. (2007), in which we relied only on photometric redshifts to identify the optical counterparts of extended X-ray emission. We revised the catalog with an efficient group-identification algorithm, demonstrated by Bielby et al. (2010) and Finoguenov et al. (2010) to the massive COSMOS data set. We give the concrete details in A. Finoguenov et al. (in preparation), and here we only briefly outline our algorithm.

On the mosaic of coadded XMM and Chandra images, cluster candidates are first identified as extended sources using a classical wavelet-transform technique of the removal of point sources (Finoguenov et al. 2009). Next, we look for any cluster red sequence around the extended X-ray sources using the deep optical–IR data. For this red-sequence search, we constructed a model red sequence using a recipe by Lidman et al. (2008), and quantified the significance of a red sequence around an extended X-ray source at a given redshift in the following manner:

- We extract galaxies located within 0.5 Mpc (physical) from the X-ray center and have $|z_{\rm phot} - z| < 0.1$, where $z_{\rm phot}$ is the photometric redshift of a galaxy and z the redshift at which we want to quantify the red sequence.
- We count galaxies with weights according to their spatial locations from the X-ray center and to their locations on a color–magnitude diagram. Bright red galaxies located at the center have the highest weight.
- We compare the count with the average count and its dispersion, which are derived by placing apertures of the same size at random positions in the COSMOS field, to quantify the significance of the red sequence.
- We repeat the above procedure at $0 < z < 2.5$ to identify peaks of the red sequence signals.
- Finally, we visually inspect all of the significant peaks, and assign redshift and confidence flags to the X-ray source.

In the first procedure, we make use of the excellent photometric redshift in the COSMOS field (Ilbert et al. 2009) to efficiently eliminate any fore-/background contamination. In the second step, we change the filter combinations to compute colors with the redshift. We have to make a compromise between the depth of data and the filter combination to probe similar rest-frame wavelengths at different redshifts, but we always straddle the 4000Å break, which is a sensitive feature of star formation. To be specific, we use the following color–magnitude diagrams:

- $0.0 < z < 0.3 : u - r$ vs. r
- $0.3 < z < 0.6 : B - i$ vs. i
- $0.6 < z < 1.0 : r - z$ vs. z
- $1.0 < z < 1.5 : i - K_{\rm S}$ vs. $K_{\rm S}$
- $1.5 < z < 2.5 : z - 3.6\,\mu$m vs. $3.6\,\mu$m

Finally, all of the significant red-sequence signals are visually inspected, and the group redshifts and confidence flags are assigned. We use 20000 redshifts from zCOSMOS (Lilly et al. 2007) to help us to identify the systems and obtain spectroscopic redshifts of them in this final identification procedure. Details of the confidence flags will be described in A. Finoguenov et al. (in preparation) but, in short, we give FLAG = 1 to groups that are unambiguously confirmed by spectroscopic redshifts, and the X-ray centroid is reliably determined by high-significance X-ray fluxes. FLAG = 2 is for spectroscopically confirmed groups whose X-ray center can potentially be off (up to 30″) due to low fluxes or to blending with other sources; the locations of the optical counterparts were used in the centroid determinations. We have confirmed that these uncertain centroids do not affect our results, as we discuss below. FLAG = 3 groups are likely to be real groups, but they have not yet been spectroscopically confirmed. The catalog contains 215 groups with FLAG = 1, 2, or 3, of which 195 are at $z < 1$. We note that $\sim$90% (175 out of 195) of the groups at $z < 1$ are spectroscopically confirmed (i.e., FLAG = 1 or 2). We did not use FLAG = 3 groups in the present work, but we have confirmed that our results do not change if we include them.

2.3. Group Members from zCOSMOS

We define group membership using the X-ray group catalog made above and the spectroscopic redshifts from zCOSMOS. In this work, we apply the following selection criteria to study the dependence of galaxy properties on the environment:

1. We use spectroscopically confirmed groups at $0.5 < z < 1.0$ with masses of between $3 \times 10^{13}\,M_{\odot}$ and $7 \times 10^{13}\,M_{\odot}$.
2. We define group members as galaxies with high-confidence spectroscopic redshifts from zCOSMOS and located within $< 2\sigma$ and $< R_{200}$ from the group centers, where σ is the line-of-sight velocity dispersion and R_{200} is the virial radius of a group within which the mean interior density is 200 times the critical density of the universe at the group redshift.

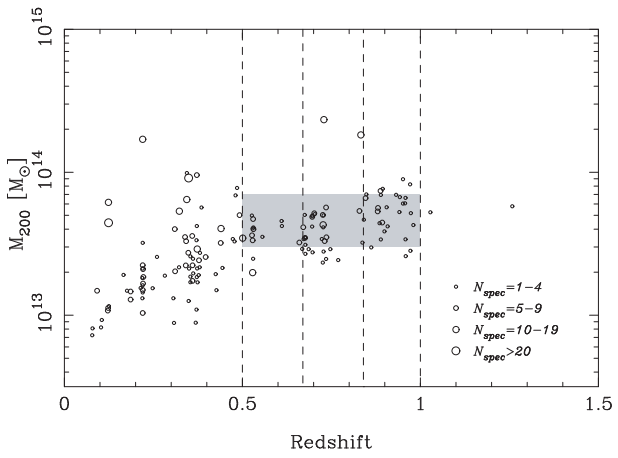

Fig. 1. M_{200} of groups measured from X-rays plotted against redshift. We used groups with high-confidence flags only. We made three redshift bins ($0.5 < z < 0.67$, $0.67 < z < 0.84$, and $0.84 < z < 1.00$), as indicated by the vertical dashed lines, where we have the [O II] line in the spectral wavelength range, and the groups are not strongly affected by fringes in the spectra. In order to minimize the group-mass dependence of galaxy properties, we use a narrow mass range such as is defined by the shade in this work. The sizes of symbols correlate with the number of spectroscopic members.

The first criterion is on groups, themselves. We want to reduce spurious groups that go into the analysis. For this, we use groups with flag 1 or 2. As mentioned above, they are spectroscopically confirmed groups. We then restrict the sample to $0.5 < z < 1.0$, as shown in figure 1. This redshift selection is made to have the [O II] emission within our spectral range. The line is not available at $z < 0.5$, and we could in principle use Hα to fill that redshift range. However, these two lines vary in their sensitivities to star formation and AGN (e.g., Hα is much more robust to extinction), and it is hard to make a fair comparison between [O II] emitters and Hα ones. We do not include the $z < 0.5$ groups in order to perform a robust analysis. We do not include $z > 1$ groups either, since extremely strong fringes in the VIMOS spectra decrease the success rate in redshift determinations of passive galaxies at $z > 1$, making any spectral analysis at $z > 1$ difficult.

In addition to the redshift criterion, we impose a group-mass threshold. As shown by previous studies (e.g., Tanaka et al. 2005; Poggianti et al. 2006; Koyama et al. 2007), galaxy properties depend on the group mass. In order to eliminate any strong group-mass dependence, and to extract evolutionary trends, we use groups with masses (M_{200}, which is the mass contained inside R_{200}) of between $3 \times 10^{13}\,M_\odot$ and $7 \times 10^{13}\,M_\odot$, as shown in figure 1. Note that M_{200} is derived from the X-ray scaling relation calibrated by weak-lensing mass estimates (Leauthaud et al. 2010). We still have a weak mass tendency within the narrow mass range in the sense that we tend to have more massive systems at higher redshifts. This bias *weakens* any evolutionary trends because more massive groups tend to be more evolved. If we had a flat group-mass distribution at $0.5 < z < 1.0$, we would have observed stronger evolutionary trends than those shown below.

The second criterion is the definition of group members. In this work, we use galaxies with highly confident spectroscopic redshifts from zCOSMOS. Specifically, we use galaxies with classes 4's, 3's (including 14's and 13's), 2.5, 2.4, 9.5, 9.4, and 9.3. For details of classes, refer the reader to Lilly et al. (2009).

To define group membership, we first estimate M_{200} from the X-rays. From this, we evaluate the velocity dispersions (σ) and virial radii (R_{200}) of the groups, while assuming that they are virialized (Carlberg et al. 1997). Since most group galaxies are observed lying within $\sim R_{200}$ in the local universe (Gómez et al. 2003; Tanaka et al. 2004), we define group members as those within R_{200} of the center. The center of groups with FLAG $= 2$ can be uncertain, but this is not a major concern in our analysis, because a typical R_{200} of these groups is 2.5 times larger than the maximum positional uncertainty of 30″. We checked the robustness of our results by perturbing the center of the FLAG $= 2$ groups with a Gaussian function with $\sigma = 30''$, and repeated all of the analysis in this paper. We observed no appreciable changes in our results. For the line-of-sight separation, we applied $<2\sigma$ of the redshift center of groups. Galaxies that do not belong to any groups are defined as field galaxies. In total, we have 7549 galaxies with high-confidence redshifts at $0.5 < z < 1$, of which 246 are in groups satisfying the above criteria. We further apply a stellar-mass cut to the galaxies listed in the next section; the total numbers of galaxies for the field and group environments used in the main analyses were 1574 and 96, respectively.

3. Galaxy Populations in the X-Ray Groups at $0.5 < z < 1.0$

3.1. Color–Mass Diagram and the Fraction of Red Galaxies

We base our analysis on the group and member catalogs described in section 2, and consider the properties of galaxies as functions of the redshift and the environment (i.e., group vs. field). To provide an overview of the properties of galaxies in our catalog, we show a rest-frame $u - r$ color vs. stellar mass diagram in figure 2. The rest-frame color and stellar mass were derived by Bolzonella et al. (2010) by fitting model templates from Bruzual and Charlot (2003), that adopted the Chabrier initial mass function (Chabrier 2003), to the photometry. A typical error in our stellar mass estimates is ~ 0.2 dex (see Bolzonella et al. 2010 for details). Before we discuss the plot, let us introduce our definition of (**a**) red/blue galaxies and (**b**) [O II] emitters.

(a) We divided galaxies into red and blue galaxies by their rest-frame $u - r$ color. We performed a biweight fit to the red sequence in groups at $0.67 < z < 0.84$, where we observed the most prominent red sequence due to the largest number of group galaxies we have there. We then shifted it by $\Delta(u - r) = -0.3$, shown as the slant dashed line in figure 2, to separate the two populations. The amount of the shift was motivated to give a reasonable separation between the [O II] emitters and non-[O II] emitters (see below for their definitions). We have confirmed that our conclusions are insensitive to a small change in the amount of the shift. We made correction for the color evolution of the red sequence in the other bins using an instantaneous burst model formed at $z_f = 3$ from Bruzual and Charlot (2003). As can be seen in the figure, the color threshold is bluer at higher redshift.

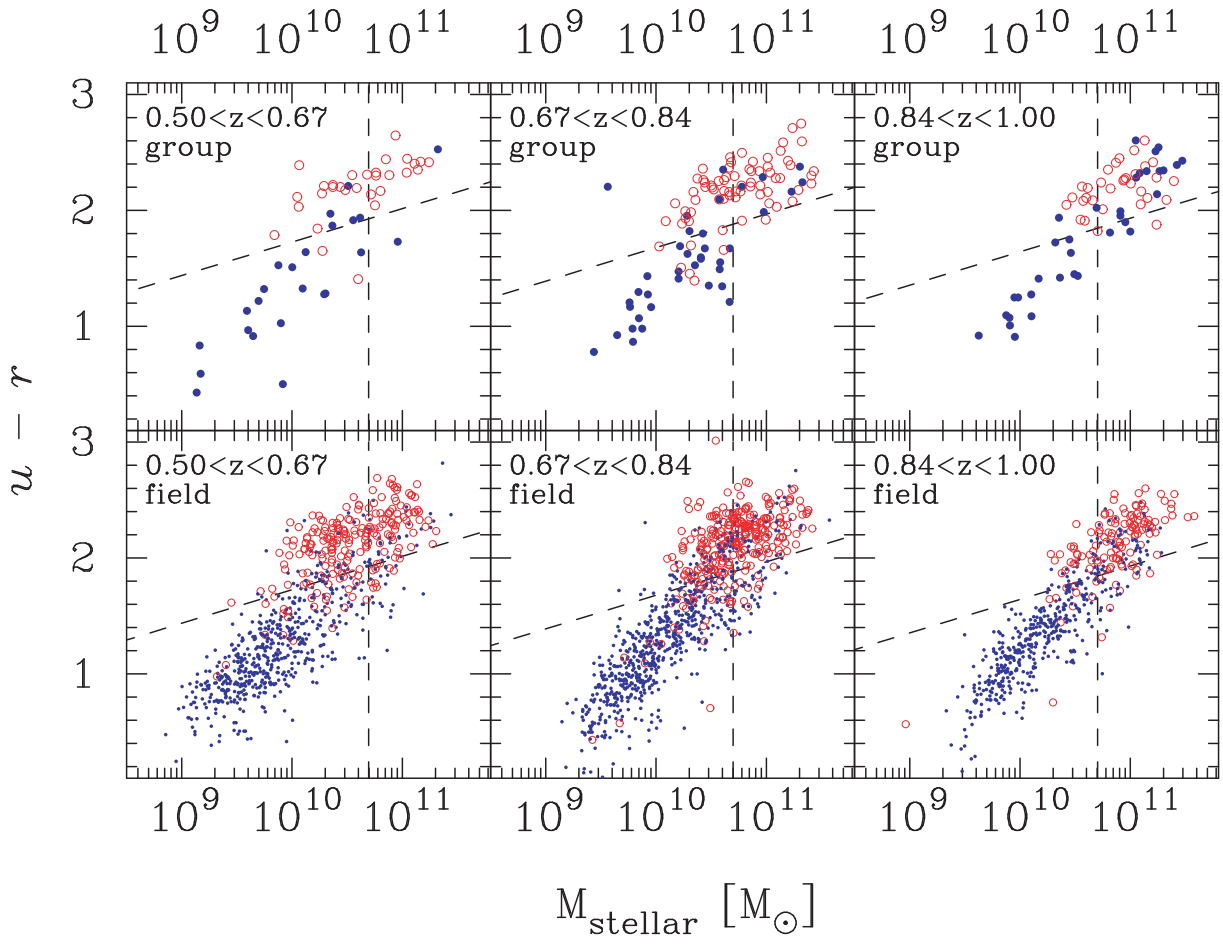

Fig. 2. Rest-frame $u-r$ color plotted against stellar mass. The top panels show the group galaxies and the bottom panels show the field galaxies. The panels are split in three redshift bins. The filled and open symbols show galaxies with and without significant [O II] emission (EW[O II] < -5 Å at $> 2.3\sigma$), respectively. The vertical dashed lines are our mass threshold, which defines the stellar mass-limited galaxy sample. We separate red and blue galaxies using the slanted dashed line. For clarify, we plot only one third of the field galaxies.

(b) We also used [O II] emission to characterize the galaxy properties. We used the equivalent width (EW) of [O II] measured by F. Lamareille et al. (in preparation). Line detections below 1.15σ were considered to be fake, and here we adopt a conservative significance threshold of 2.3σ to ensure that the line was securely detected. We define galaxies with EW[O II] < -5 Å detected at $> 2.3\sigma$ as [O II] emitters, and the other galaxies as quiescent. Note that we use a negative sign for emission.

Let us go back to figure 2. It is immediately clear that the most massive galaxies tend to be red, and many of them do not show any sign of active star formation. Galaxies with no significant [O II] form a definite sequence of red galaxies. Interestingly, some of the red galaxies show significant [O II] emission despite their red colors. In contrast to massive galaxies, low-mass galaxies are predominantly blue [O II] emitters. This is due to a bias introduced by the flux limit of the survey. The I band, with which spectroscopic targets are selected in zCOSMOS, samples bluer light in rest-frame at higher redshifts, and we miss low-mass red galaxies, resulting in a strong bias toward blue, star-forming galaxies.

It is hard to interpret figure 2 due to the strong selection bias. We apply a stellar-mass cut in each redshift bin to construct a stellar mass-limited sample in order to study evolutionary trends. We have to make correction for the mass evolution in each redshift bin, but we cannot track the mass evolution of individual galaxies, which depends on their star formation and merger histories. Here, we simply apply a correction for the passive evolution using the same passive evolution model as is used for the color evolution. We can reach $\sim 5 \times 10^{10}\,M_\odot$ galaxies at $z = 1$ in zCOSMOS, although the redshift success rate drops to 70% (see figures 2 and 10 of Lilly et al. 2009). Cucciati et al. (2010) and Iovino et al. (2010) applied a conservative cut of $10^{11}\,M_\odot$, but for the purpose of the paper we do not need to be 100% complete, and we apply stellar mass thresholds of $4.95 \times 10^{10}\,M_\odot$ at $0.5 < z < 0.67$, $5 \times 10^{10}\,M_\odot$ at $0.67 < z < 0.84$, and $5.05 \times 10^{10}\,M_\odot$ at $0.84 < z < 1$. We note that our conclusions do not change if we adopt a conservative mass cut of $10^{11}\,M_\odot$, although the statistics become poor. Balogh et al. (2011) reported on an abundant population of green valley galaxies in groups at $0.85 < z < 1$. We do not observe strong evidence for an increased amount of green galaxies in figure 2, but we cannot probe such low-mass galaxies that they did ($10^{10.1}\,M_\odot$).

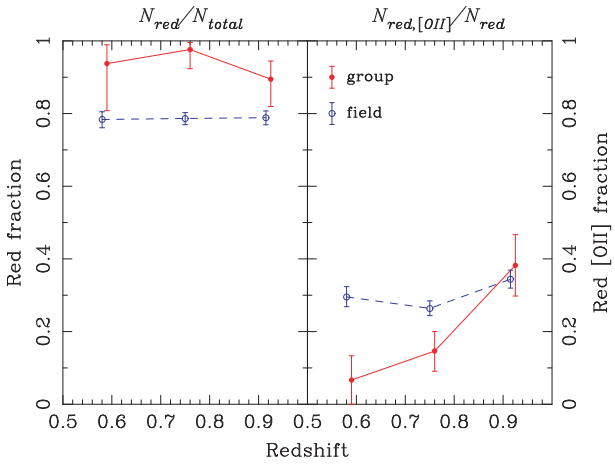

Fig. 3. Left: Fraction of red galaxies plotted against redshift. Here, we use the stellar mass-limited sample in both the group and field environments. The filled and open symbols show the group and field samples, respectively. They are slightly shifted horizontally to avoid overlapping. The error bars show the 68% confidence interval (Gehrels 1986). Right: Fraction of [O II] emitters among red galaxies against redshift.

We plot the fraction of red galaxies as a function of redshift in figure 3 using the stellar mass-limited sample. The fraction of massive red galaxies remains constant in the range of the explored redshift both in groups and in the field. An interesting trend in figure 3 is that the red fraction is always higher in groups than in the field, showing a clear environmental dependence of galaxy colors at $0.5 < z < 1$. This may appear to be inconsistent with previous studies (e.g., Cucciati et al. 2010; Iovino et al. 2010); we discuss this in subsection 4.1. While we do not see strong color evolution, we see a clear increase in the fraction of [O II] emitters among red galaxies at high redshifts, as shown in the right panel of figure 3. As mensioned earlier, our group sample is biased toward more massive groups at higher redshifts, which weakens any evolutionary trends. Also, due to the nature of a mass-limited sample, spectra at higher redshifts have lower signal-to-noise ratios. We tend to miss weak [O II] emissions at higher redshifts, which weakens the trend that we see here.[1] The real evolutionary trend should be stronger than the observed one in figure 3.

The fraction of red [O II] emitters remains fairly constant with redshift in the field, while it evolves very fast in groups. The fractions become indistinguishable in between groups and the field in the highest redshift bin. These red [O II] emitters must have dusty star-formation activities and/or AGN activities. This is a sort of evolution that cannot be revealed by broad-band photometry, demonstrating the power of large spectroscopic surveys.

[1] One might suspect that we tend to miss quiescent red galaxies at $z \sim 1$ due to the busy OH lines, which might be driving the observed increase of red galaxies with [O II] emission which is easily identified. However, as discussed in subsection 3.2, red [O II] emitters increases with stellar mass in the highest redshift bin. This is a different trend from what is expected from the redshift determination bias, because we do not miss massive (bright), passive galaxies in spite of the presence of busy OH lines. Therefore, the observed trend is unlikely due to an observational bias.

3.2. *Stellar Mass and Redshift Dependence of the [O II] Emitters*

Essentially all galaxy properties correlate with the stellar mass. It would be important to show that the higher red fraction in groups shown in figure 3 is not due to the environmental dependence of the stellar-mass function, such that groups host a larger fraction of massive galaxies, which increases the red fraction because massive galaxies tend to be red. We plot in figure 4 the fraction of red galaxies as functions of the stellar mass and the redshift. We find that the red fraction tends to be higher in groups than in the field at a given stellar mass, although the error bars often overlap. The difference between groups and the field is particularly clear at $0.67 < z < 0.84$, where we have a prominent large-scale structure (Guzzo et al. 2007). The poor statistics do not allow us to conclude that the groups show a higher red fraction at a given stellar mass, but the systematically higher fraction suggests that the observed high red fraction in groups in figure 3 is not entirely due to the dependence of the stellar-mass function on the environment. We note that George et al. (2011) showed that the red fraction is higher in groups than in the field at a given stellar mass, based on the same X-ray group catalog and on the photometric data in COSMOS.

Similarly, it would be interesting to look at the stellar-mass dependence of the [O II] emitters on the red sequence. We plot in figure 5 the fraction of the red [O II] emitters as a function of the stellar mass. In the field, the fraction of the red [O II] emitters does not strongly depend on mass above the mass threshold. The overall fraction does not show a marked increase with redshift either. On the other hand, the fraction in groups increases at higher redshift, and in the highest redshift bin, the fraction of [O II] emitters seems to increase with mass above the mass cut. Although the statistics are poor, the fractions of groups and the field have contrasting trends. It seems that the increase of [O II] emitters in groups at high redshift is stronger for more massive galaxies.

A high fraction of [O II] emitters at $z \sim 1$ has already been observed by several authors. Nakata et al. (2005) found the fraction of EW[O II] < -10 Å galaxies at $0.8 < z < 1$ to be $\sim 0.45 \pm 0.15$. Their sample is not stellar mass limited, and we cannot make a fair comparison between our sample and theirs. However, if we apply the same selection of EW[O II] < -10 Å to our sample, we obtain a consistent fraction of 0.31 ± 0.07. Poggianti et al. (2006) showed the high fraction (very roughly 50%) in groups and clusters at $0.4 < z < 0.8$. If we apply EW[O II] < -3 Å, as done in Poggianti et al. (2006), we obtain a consistent fraction. A similarly high fraction of [O II] emitters in groups at higher redshift ($z = 1.2$) is reported by Tanaka et al. (2009). If we apply our definitions of the [O II] emitters and the stellar mass cut to their sample, we find that the fraction of massive [O II] emitters is 0.47 ± 0.22. We should be careful about this face value, since their sample was taken from optically selected groups, and the targets for spectroscopy were photo-z selected, which potentially introduces biases into the sample. However, this high fraction of [O II]-emitting galaxies in groups taken from completely different sample is reassuring. Unfortunately, their sample is not large enough to constrain the mass dependence of the [O II] emitters.

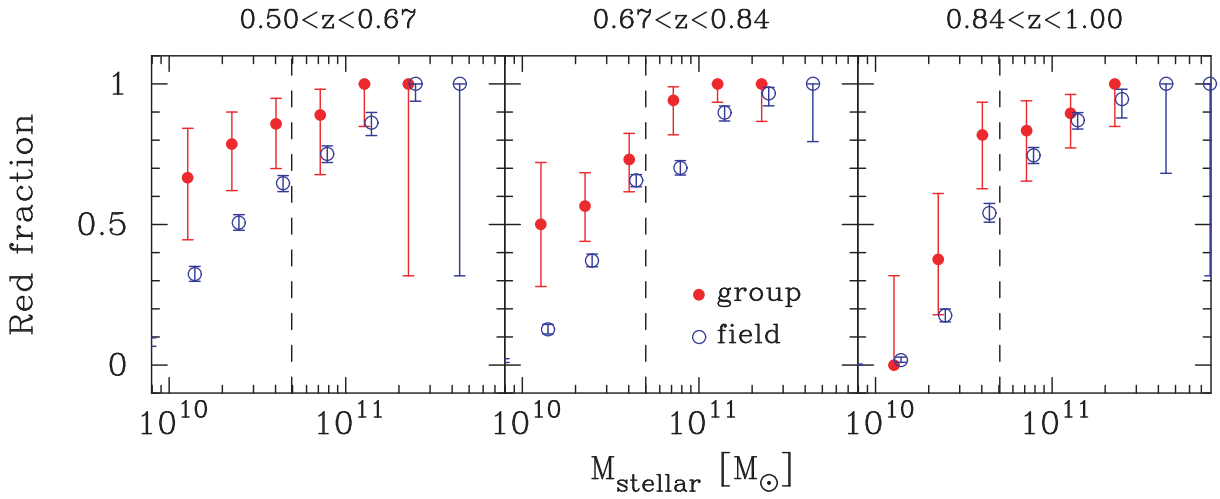

Fig. 4. Fraction of red galaxies as a function of stellar mass in the three redshift bins. The filled and open circles are the group and field galaxies, respectively. The vertical dashed line is the mass threshold, which defines the stellar mass-limited sample. The error bar shows the 68% confidence interval.

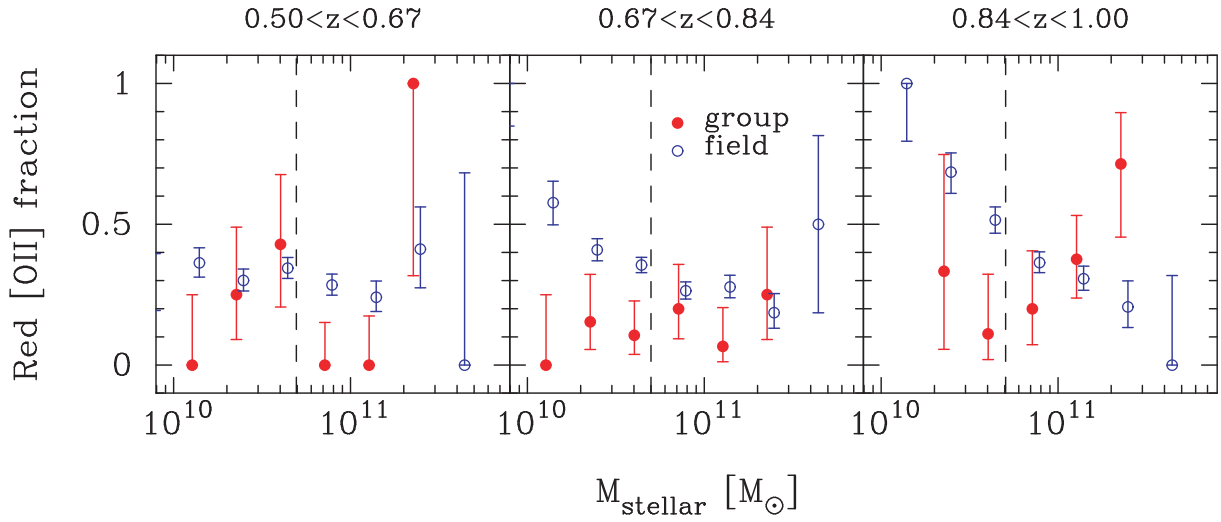

Fig. 5. Fraction of red [O II] emitters as a function of stellar mass. The same as in figure 4, the panel is split into the three redshift bins. The vertical dashed line is the stellar mass cut. The error bar shows the 68% confidence interval.

Not only the fraction of red [O II] emitters, but the strengths of the emission seem to increase with redshift, as shown in figure 6. Field galaxies in the median EW[O II] do not change appreciably with the redshift. On the other hand, group galaxies seem to show a larger EW[O II] tail at higher redshifts. The distributions of EW[O II] in groups at $0.67 < z < 0.84$ and $0.84 < z < 1$ show a null probability of 3% from the Mann–Whitney U test. This increase in EW[O II] would not be too surprising given the rapid increase in the fraction of [O II] emitters observed in figure 3, which is statistically significant. We have only one red [O II] emitter at $0.50 < z < 0.64$, and we cannot apply any statistical tests there. In contrast to groups, field galaxies do not show any strong evolutionary trends; the Mann–Whitney test gives null probabilities of 33% between $0.50 < z < 0.64$ and $0.67 < z < 0.84$ and of 47% between $0.67 < z < 0.84$ and $0.84 < z < 1$. Wilman et al. (2008) showed that $\sim$50% of galaxies with $10^{11}\,M_{\odot}$ in $z \sim 0.4$ groups show infrared-flux excess, which can be due to star formation and/or AGN. The observed low frequency of the [O II] emitters compared to the infrared detections may be because [O II] and infrared have different sensitivities to star formation and AGN.

To sum up, we observe that the fraction of red galaxies with $> 5 \times 10^{10}\,M_{\odot}$ does not strongly evolve at $0.5 < z < 1$ in both the group and field environments, and it is always higher in groups than in the field. The most striking trend that we find is that the fraction of red [O II] emitters in groups increases at higher redshifts, while the fraction is nearly constant in the field. It seems that more massive galaxies in groups show a stronger increase in [O II]. This trend suggests that the red galaxies in groups have dusty star-formation and/or AGN activities, and the rates at which the environment suppresses such activities are different in each environment. We pursue this point in the next section.

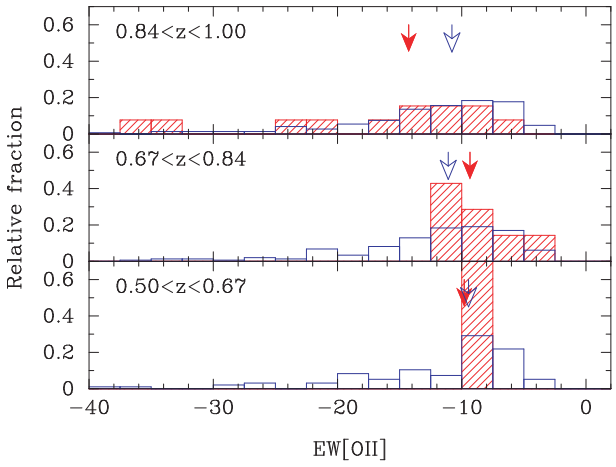

Fig. 6. Distribution of EW[O II] of red galaxies measured at $> 2.3\sigma$ in group (shaded histogram) environment and in field (open histogram) one based on the stellar mass-limited sample. The arrow points the median of the EW[O II] in each environment.

4. Discussions

4.1. Comparisons with Previous Studies

Recent large spectroscopic surveys, such as zCOSMOS (Lilly et al. 2007), DEEP2 (Davis et al. 2003), and VVDS (Le Fèvre et al. 2005), have enabled statistical analysis of galaxies in the universe up to $z = 1$, and even beyond that. Several authors have studied the environmental dependence of galaxy properties using data from those surveys (e.g., Cucciati et al. 2006, 2010; Cooper et al. 2007, 2010; Gerke et al. 2007; Iovino et al. 2010). However, the results from those papers are not always consistent. In particular, results on the color–density relation at $z \sim 1$ and their interpretations seem to be controversial.

In fact, our finding that the fraction of red galaxies depends on environment up to $z \sim 1$ does not seem to be consistent at first glance with those from Cucciati et al. (2010) and Iovino et al. (2010), who have found no strong dependence of galaxy colors on density at $z \sim 1$, based on a stellar mass-limited sample. Another finding by Iovino et al. (2010) is that the fraction of red galaxies decreases with redshift, which is not consistent either. Cooper et al. (2010) discussed differences between data sets and between methods by which analyses were made in the literature. However, we use basically the same data set as Cucciati et al. (2010) and Iovino et al. (2010), and the observed differences appear to be at odds. Here, we attribute the cause of the differences to (i) definitions of environments and (ii) definitions of red galaxies.

There is a fair amount of evidence that galaxy properties depend on the mass of groups and clusters at high redshifts (e.g., Tanaka et al. 2005; Poggianti et al. 2006; Koyama et al. 2007). In this paper, we use X-ray selected groups, while most of the previous papers from large spectroscopic surveys are based on galaxy groups (or galaxy densities) identified by using spectroscopically observed galaxies. There are the pros and cons of these environment definitions, but the advantage of the X-ray groups is that our environment is mass-selected. As mentioned earlier, 90% of the groups at $z < 1$ in COSMOS are spectroscopically confirmed, and we probably sampled the group-mass environments well in this study. A further comparison between optical and X-ray groups will be made in A. Finoguenov et al. (in preparation).

A disadvantage would be that we cannot identify very low-mass groups that are below our X-ray detection limit, while optical group algorithms can do. We suspect that these low-mass groups would be the primary cause of the difference between our results and those of Cucciati et al. (2010) and Iovino et al. (2010). Iovino et al. (2010) showed that optically poor groups tend to exhibit a lower red fraction than optically rich ones. Poor groups are more numerous than rich ones, and they dominate the group sample, which results in a smaller difference in the fraction of red galaxies between groups and the field. The explored group-mass ranges could account for the difference in the dependence of the red fraction on the environment between the previous studies and ours.

Another cause of the difference is that our definition of red galaxies is different from that adopted in Iovino et al. (2010). They adopted a color threshold of $U - B = 1$ regardless of the redshift and the stellar mass of galaxies, while we account for the tilt of the red sequence with respect to stellar mass, and also for the passive evolution. We have confirmed that the red fraction decreases at higher redshifts if we adopt the same definition as theirs. We prefer accounting for the tilt and passive evolution to defining red/ blue galaxies in this paper. The above two reasons are likely to be the primary causes of the somewhat difference between our results and the previous authors'.

Gerke et al. (2007) and Cooper et al. (2007) also suggested that the red fraction decreases with redshift in high-density environments. This might be due to the selection of galaxies. They applied a rest-frame B-band magnitude cut, not a stellar mass cut. The B-band magnitude cut introduces a strong bias toward star-forming galaxies, which could result in a lower red fraction at higher redshifts.

We note that there is the nonzero possibility that we miss groups dominated by blue galaxies because we used the red sequence finder in the group-identification process, which could possibly enhance the difference between groups and the field. However, our technique uses the contrast in the red sequences of groups and the field, and we do not actually require a higher fraction of red galaxies in groups. Even if groups have the same red fraction as the field, we can identify them as long as they show an overdensity. We miss only groups in which the fraction of red galaxies is significantly lower than that in the field. It is unlikely that such very blue groups are so abundant that they change our results significantly, because we have identified $\sim$90% of all X-ray group candidates at $z < 1$ with great confidence; they exhibit a clearer red sequence when compared with field galaxies.

Recently, Koyama et al. (2011) reported on Hα narrow-band imaging of a $z = 0.4$ cluster. They found that groups exhibit a higher fraction of Hα emitters than the field does, which is in contrast to our finding given in the right panel of figure 3. There are a number of differences in the explored stellar mass range, observing technique, emission line used, and emission-line sensitivity. These differences do not permit detailed comparison with our results.

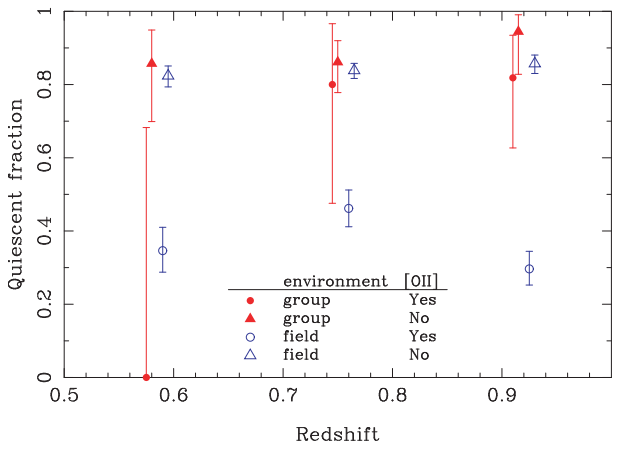

Fig. 7. Fraction of quiescent galaxies with $(NUV-r)_{\rm dered} > 3.5$ among the red galaxies in groups and the field with/without [O II] plotted against redshift. The meaning of the symbols is shown in the plot. The error bar shows the 68% confidence interval.

4.2. *Origin of the [O II] Emission—Star Formation vs. AGN*

The fraction of red [O II] emitters increasing with redshift must be due to increasing dusty star-formation activities and/or AGN activities. Recent studies of $z > 1$ clusters also reported on an increased rate of emission-line galaxies in clusters than in lower redshift clusters (e.g., Hayashi et al. 2010, but see also Bauer et al. 2011). However, this trend is not yet established, and it is not clear whether the emission line originates from star formation or AGN activities, either?

Let us first ask if the [O II] emission is due to dusty star formation. We look at the $(NUV-r)_{\rm dered}$ color of the [O II] emitters taken from Ilbert et al. (2009). The $(NUV-r)_{\rm dered}$ color is a reddening-corrected color of galaxy templates used for photometric redshift estimates (i.e., the raw template color without dust extinction) using 30-band photometry. This is sensitive to ongoing star formation, as shown by Ilbert et al. (2010). We adopt a threshold of $(NUV-r)_{\rm dered} = 3.5$ to separate quiescent galaxies from star-forming galaxies (Ilbert et al. 2010), and plot the fraction of quiescent galaxies in figure 7. Since the color from Ilbert et al. (2009) is based on photometric redshifts, we have used galaxies with correct photometric redshifts ($|z_{\rm phot} - z_{\rm spec}| < 0.05$). We note that this analysis is essentially equivalent to the popular two-color diagnostics used to separate quiescent red galaxies from dusty ones (Wolf et al. 2005, 2009). However, instead of using only 2 colors, we here make use of 30-band photometry, which gives a fine sampling of galaxy SEDs ranging over a wide wavelength to discriminate quiescent galaxies from dusty star-forming ones.

Let us start with red galaxies without significant [O II] emission, shown by the open and filled triangles in figure 7. The fractions of these galaxies are very high, as expected from the absence of [O II]. The stellar population of these galaxies is typically old, and there is no significant difference between groups and the field. That is, if red galaxies exhibit no [O II], they are dominated by old stellar populations, regardless of the environment. Now, we turn our attention to the red [O II] emitters. The fraction of the red [O II] emitters of quiescent galaxies in the field (open circle) is relatively low (30%–40%), suggesting that more than a half of them are not quiescent, and are probably undergoing dusty star formation. In contrast, the red [O II] emitters in groups (filled circle) show a very high fraction, even at high redshifts; it is as high as those without [O II] emission. This suggests that red [O II] emitters in groups are dominated by old stellar populations despite the [O II] emission. In figure 3, we can observe a sharp increase in the fraction of red [O II] emitters in high-redshift groups, but the fraction of quiescent galaxies does not show a corresponding decrease. There is no clear evidence for increased dusty galaxies in the red [O II] emitters in groups. Instead, figure 7 favors the AGN origin.

Let us then consider from a wider point of the view and ask if the [O II] emission comes from AGNs. In the redshift range under study, we cannot use strong emission-line diagnostics such as that proposed by Baldwin, Phillips, and Terlevich (1981) to identify AGNs, since Hα line migrates to near-IR. Here, we use another way of identifying AGNs —X-rays—and quantify how AGNs populate in the redshift range studied here. We used the Chandra point-source catalog (Elvis et al. 2009) and applied an X-ray luminosity cut of $L_{0.5-10\,{\rm keV}} > 10^{43}\,{\rm erg\,s^{-1}}$, that is nearly complete up to $z = 1$. In the field, an X-ray detection rate of the red [O II] emitters seems to increase in the highest redshift bin: 0.04 ± 0.03, 0.03 ± 0.02, and 0.13 ± 0.04 from low to high redshift bins. However, we have detected no red [O II] emitters in groups in X-rays: $0.00^{+0.68}_{-0.00}$, $0.00^{+0.32}_{-0.00}$, and $0.00^{+0.17}_{-0.00}$ from low to high redshifts.

Most of the red [O II] emitters in groups were not detected in X-rays (only 2 are detected, but they have luminosities below the cut applied above). We performed a stacking analysis of those undetected sources in the soft band with care to remove the extended component (Finoguenov et al. 2009). By stacking 9 objects that were not individually detected, we measured an average luminosity of $2.8 \times 10^{-17}\,{\rm erg\,s^{-1}\,cm^{-2}}$ in 0.5–2 keV, which is translated into $2.7 \times 10^{40}\,{\rm erg\,s^{-1}}$ at $z = 0.5$ and $1.5 \times 10^{41}\,{\rm erg\,s^{-1}}$ at $z = 1$. This luminosity level can be explained by both low-luminosity AGN and star-formation origins. We cannot constrain the AGN fraction in groups with X-rays.

X-rays, unfortunately, do not put any constraint on the AGN or dusty star-formation origin, but the robust photometric analysis based on the 30 photometric bands presented above seems to lend support to the AGN origin of the [O II] emission, although the statistics are poor. The stellar population of the red [O II] emitters in groups is old, and there is no hint of strong ongoing star formation in those galaxies. The observed [O II] emission is unlikely due to star formation, and its origin is most probably AGNs. Recently, Tanaka (2012a, 2012b) presented a new method of identifying AGNs based on a very simple idea of comparing the emission-line luminosity that is expected to be due to star formation with an observed luminosity. They derived the expected luminosity due to star formation from the stellar continua. Our analysis based on the $(NUV-r)_{\rm dered}$ color is essentially the same as theirs. We expect very weak (or even no) emission lines from the 30-band photometry, which mostly probes the stellar continua, but we actually observe clear emission lines in the spectra. Although

a detailed analysis is beyond the scope of this paper, it is likely that these objects harbor AGNs.

A possibility of weak AGNs in groups is supported by the recent work of Lemaux et al. (2010), who performed near-IR spectroscopy of galaxies dominated by old stellar population, but having [O II] emission in clusters of $z = 0.8$ and 0.9. They found that a significant fraction of them ($\sim$70%) harbor AGNs. It would not be surprising if a large fraction of the red [O II] emitters in our high redshift groups are AGNs, since they have photometric properties similar to those studied in Lemaux et al. (2010). However, other authors reported on increased dusty star-formation activities in groups at high redshifts (e.g., Koyama et al. 2008, 2010; Kocevski et al. 2011). Tanaka et al. (2009) found that group galaxies at $z \sim 1.2$ show weak Hδ absorptions, and they speculated that the absorption might be due to the large extinction. Post-starburst galaxies might favor groups (Poggianti et al. 2009). Vergani et al. (2010) also reported that post-starburst galaxies prefer high-density environments based on the zCOSMOS data. Recently, Hayashi et al. (2011) observed that both AGN and star formation take place in a $z = 1.4$ cluster.

Under this controversial situation, it is probably fair to say that the origin of the emission line is still unclear at this point. It may be that both dusty star-formation and AGN activities increase at high redshifts, and there is a strong cluster-cluster variation. Any conclusion on the origin of [O II] emission needs to be drawn from a larger statistical sample of groups at $z \gtrsim 1$. An extensive near-IR spectroscopy targeting Hα and [N II] lines of red [O II] emitters in groups to perform emission-line diagnostics, such as that proposed by Baldwin, Phillips, and Terlevich (1981), would be a promising method. Also, a newly developed AGN identification method by Tanaka (2012a, 2012b) is effective as well because it requires only [O II] and/or [O III]. Obviously, deep Chandra observations are very helpful as well. Using these techniques, we first have to discriminate AGNs from star formation in order to interpret the recent observations that distant groups and clusters tend to show an increased rate of emission-line galaxies.

5. Summary

We have presented photometric and spectroscopic analyses of zCOSMOS galaxies at $0.5 < z < 1$. Unlike most of the previous studies, we define the mass-selected environments to study the dependence of galaxy properties on the environment. This is one of the most important features of the present work. Previous studies have shown that galaxy properties depend on the mass of groups and clusters. These studies clearly show that the environment needs to be defined by mass.

We have found that the fraction of red galaxies is always higher in groups than in the field at $0.5 < z < 1$, and it does not strongly change in this redshift range. Our results might appear to be inconsistent with previous studies from zCOSMOS, but we have argued that this is due to the different definitions of the environment and red galaxies. The most important finding of this paper is that the fraction of [O II] emitters on the red sequence in groups increases at higher redshifts, while the fraction in the field does not show any significant evolution. The increased red [O II] emitters in groups must be due to increased dusty star-formation activities and/or to increased AGN activities. We have considered the two possibilities by using the 30-band photometry and X-ray data. While the X-ray data put no strong constraint upon them, the 30-band photometry suggests that the stellar population of the [O II] emitters in groups is old, and there is no hint of enhanced dusty star-forming activities. This lends support to increased AGN activities.

Recent observations often report on a high fraction of emission line galaxies in distant groups and clusters. The question is now where the emission comes from. We have obtained evidence for the AGN origin, and the recent near-IR spectroscopic work also favors it. However, our overall statistics are poor, and some of the previous studies seem to favor the dusty star-formation origin. Obviously, more observations are needed to settle the issue.

This work was supported by World Premier International Research Center Initiative (WPI Initiative), Ministry of Education, Culture, Sports, Science and Technology of Japan and also in part by JSPS. KAKENHI No. 23740144. This work is based on observations undertaken at the European Southern Observatory (ESO) Very Large Telescope (VLT) under the Large Program 175.A-0839. We would like to thank an anonymous referee for useful comments, which helped us to improve the paper.

References

Aihara, H., et al. 2011, ApJS, 193, 29
Baldry, I. K., Balogh, M. L., Bower, R. G., Glazebrook, K., Nichol, R. C., Bamford, S. P., & Budavari, T. 2006, MNRAS, 373, 469
Baldwin, J. A., Phillips, M. M., & Terlevich, R. 1981, PASP, 93, 5
Balogh, M. L., et al. 2011, MNRAS, 412, 2303
Balogh, M. L., Morris, S. L., Yee, H. K. C., Carlberg, R. G., & Ellingson, E. 1997, ApJ, 488, L75
Bauer, A. E., Grützbauch, R., Jørgensen, I., Varela, J., & Bergmann, M. 2011, MNRAS, 411, 2009
Bielby, R. M., et al. 2010, A&A, 523, A66
Blanton, M. R., et al. 2003, ApJ, 594, 186
Blanton, M. R., Eisenstein, D., Hogg, D. W., Schlegel, D. J., & Brinkmann, J. 2005, ApJ, 629, 143
Bolzonella, M., et al. 2010, A&A, 524, A76
Bruzual, G., & Charlot, S. 2003, MNRAS, 344, 1000
Carlberg, R. G., Yee, H. K. C., & Ellingson, E. 1997, ApJ, 478, 462
Chabrier, G. 2003, PASP, 115, 763
Colless, M., et al. 2003, arXiv:astro-ph/0306581
Cooper, M. C., et al. 2010, MNRAS, 409, 337
Cooper, M. C., et al. 2007, MNRAS, 376, 1445
Cucciati, O., et al. 2006, A&A, 458, 39
Cucciati, O., et al. 2010, A&A, 524, A2
Davis, M., et al. 2003, Proc. SPIE, 4834, 161
Demarco, R., et al. 2005, A&A, 432, 381
Demarco, R., et al. 2007, ApJ, 663, 164
Doi, M., et al. 2010, AJ, 139, 1628
Dressler, A. 1980, ApJ, 236, 351

Dressler, A., et al. 1997, ApJ, 490, 577
Elvis, M., et al. 2009, ApJS, 184, 158
Fassbender, R., Böhringer, H., Lamer, G., Mullis, C. R., Rosati, P., Schwope, A., Kohnert, J., & Santos, J. S. 2008, A&A, 481, L73
Finoguenov, A., et al. 2007, ApJS, 172, 182
Finoguenov, A., et al. 2009, ApJ, 704, 564
Finoguenov, A., et al. 2010, MNRAS, 403, 2063
Fukugita, M., Ichikawa, T., Gunn, J. E., Doi, M., Shimasaku, K., & Schneider, D. P. 1996, AJ, 111, 1748
Gehrels, N. 1986, ApJ, 303, 336
Geller, M. J., & Huchra, J. P. 1989, Science, 246, 897
George, M. R., et al. 2011, ApJ, 742, 125
Gerke, B. F., et al. 2007, MNRAS, 376, 1425
Gómez, P. L., et al. 2003, ApJ, 584, 210
Goto, T., Yamauchi, C., Fujita, Y., Okamura, S., Sekiguchi, M., Smail, I., Bernardi, M., & Gomez, P. L. 2003, MNRAS, 346, 601
Guzzo, L., et al. 2007, ApJS, 172, 254
Hasinger, G., et al. 2007, ApJS, 172, 29
Hayashi, M., Kodama, T., Koyama, Y., Tadaki, K.-I., & Tanaka, I. 2011, MNRAS, 415, 2670
Hayashi, M., Kodama, T., Koyama, Y., Tanaka, I., Shimasaku, K., & Okamura, S. 2010, MNRAS, 402, 1980
Ilbert, O., et al. 2009, ApJ, 690, 1236
Ilbert, O., et al. 2010, ApJ, 709, 644
Iovino, A., et al. 2010, A&A, 509, A40
Kauffmann, G., White, S. D. M., Heckman, T. M., Ménard, B., Brinchmann, J., Charlot, S., Tremonti, C., & Brinkmann, J. 2004, MNRAS, 353, 713
Kocevski, D. D., Lemaux, B. C., Lubin, L. M., Shapley, A. E., Gal, R. R., & Squires, G. K. 2011, ApJ, 737, L38
Kodama, T., Smail, I., Nakata, F., Okamura, S., & Bower, R. G. 2001, ApJ, 562, L9
Koekemoer, A. M., et al. 2007, ApJS, 172, 196
Koyama, Y., et al. 2008, MNRAS, 391, 1758
Koyama, Y., Kodama, T., Nakata, F., Shimasaku, K., & Okamura, S. 2011, ApJ, 734, 66
Koyama, Y., Kodama, T., Shimasaku, K., Hayashi, M., Okamura, S., Tanaka, I., & Tokoku, C. 2010, MNRAS, 403, 1611
Koyama, Y., Kodama, T., Tanaka, M., Shimasaku, K., & Okamura, S. 2007, MNRAS, 382, 1719
Leauthaud, A., et al. 2010, ApJ, 709, 97
Le Fèvre, O., et al. 2003, Proc. SPIE, 4841, 1670
Le Fèvre, O., et al. 2005, A&A, 439, 845
Lewis, I., et al. 2002, MNRAS, 334, 673
Lemaux, B. C., Lubin, L. M., Shapley, A., Kocevski, D., Gal, R. R., & Squires, G. K. 2010, ApJ, 716, 970
Lidman, C., et al. 2008, A&A, 489, 981
Lilly, S. J., et al. 2007, ApJS, 172, 70
Lilly, S. J., et al. 2009, ApJS, 184, 218
Lilly, S. J., Le Fevre, O., Crampton, D., Hammer, F., & Tresse, L. 1995, ApJ, 455, 50
Lubin, L. M., Oke, J. B., & Postman, M. 2002, AJ, 124, 1905
Mei, S., et al. 2009, ApJ, 690, 42
Nakata, F., Bower, R. G., Balogh, M. L., & Wilman, D. J. 2005, MNRAS, 357, 679
Poggianti, B. M., et al. 2006, ApJ, 642, 188
Poggianti, B. M., et al. 2008, ApJ, 684, 888
Poggianti, B. M., et al. 2009, ApJ, 693, 112
Poggianti, B. M., Smail, I., Dressler, A., Couch, W. J., Barger, A. J., Butcher, H., Ellis, R. S., & Oemler, A., Jr. 1999, ApJ, 518, 576
Postman, M., & Geller, M. J. 1984, ApJ, 281, 95
Rettura, A., et al. 2010, ApJ, 709, 512
Rosati, P., Stanford, S. A., Eisenhardt, P. R., Elston, R., Spinrad, H., Stern, D., & Dey, A. 1999, AJ, 118, 76
Scoville, N., et al. 2007, ApJS, 172, 1
Shectman, S. A., Landy, S. D., Oemler, A., Tucker, D. L., Lin, H., Kirshner, R. P., & Schechter, P. L. 1996, ApJ, 470, 172
Stanford, S. A., et al. 2005, ApJ, 634, L129
Stanford, S. A., et al. 2006, ApJ, 646, L13
Strazzullo, V., et al. 2010, A&A, 524, A17
Tanaka, M. 2012a, PASJ, 64, 36
Tanaka, M. 2012b, PASJ, 64, 37
Tanaka, M., De Breuck, C., Venemans, B., & Kurk, J. 2010b, A&A, 518, A18
Tanaka, M., Finoguenov, A., & Ueda, Y. 2010a, ApJ, 716, L152
Tanaka, M., Goto, T., Okamura, S., Shimasaku, K., & Brinkmann, J. 2004, AJ, 128, 2677
Tanaka, M., Kodama, T., Arimoto, N., Okamura, S., Umetsu, K., Shimasaku, K., Tanaka, I., & Yamada, T. 2005, MNRAS, 362, 268
Tanaka, M., Lidman, C., Bower, R. G., Demarco, R., Finoguenov, A., Kodama, T., Nakata, F., & Rosati, P. 2009, A&A, 507, 671
Tasca, L. A. M., et al. 2009, A&A, 503, 379
Vergani, D., et al. 2010, A&A, 509, A42
Whitmore, B. C., Gilmore, D. M., & Jones, C. 1993, ApJ, 407, 489
Wilman, D. J., et al. 2008, ApJ, 680, 1009
Wolf, C., et al. 2009, MNRAS, 393, 1302
Wolf, C., Gray, M. E., & Meisenheimer, K. 2005, A&A, 443, 435
York, D. G., et al. 2000, AJ, 120, 1579